OPTICS MODELLING CHALLENGES FOR THE HL-LHC

R. De Maria*, P. Bestmann, G. Dima, L. Fiscarelli, C. Petrone, V. Rude, K. Skoufaris,
European Organization for Nuclear Research, Geneva, Switzerland

Abstract

The HL-LHC will operate with very low β^* and tight alignment constraints around the upgraded ATLAS and CMS experiments. Minimizing the commissioning time required to reach the nominal will be key to achieving significant luminosity in the first years of operation. This contribution presents the status and perspectives of the solutions implemented to prepare machine models that allow us to predict, with the best possible accuracy, the orbit and optics of the machine at the start of commissioning in Run 4. In particular, it shows the status of modeling magnetic-axis deviations, the inclusion of measured magnetic transfer functions and quadrupole fringe fields in optics models, and their expected impact on residual orbit error and optics-correction convergence speed during commissioning.

INTRODUCTION

HL-LHC optics around the interaction regions at the end of luminosity leveling have large β-functions to produce a very small beam spot at the interaction point. The nominal β^* in the HL-LHC is 15 cm in both planes (achieved in one plane only in the LHC in 2026 [1]), with options to go down to 7.5 cm [2–4]. Compared with the LHC, even for the same β^*, the peak beta in the triplet is 45 % larger [5]. Nominal HL-LHC β-functions reach 22 km in the first quadrupoles close to the interaction point (in the inner triplets, MQXFA, MQXFB). Large β-functions increase the sensitivity to imperfections and nonlinear fields, making optics corrections more challenging. This paper describes the process of building an as-built operational model in Run 4 instead of a nominal one[1] and discusses the expected advantages.

MAGNETIC AXIS DEVIATIONS

Deviations of the magnetic axis generate 1) unwanted orbit errors proportional to the transverse offsets of the magnetic axis (the position at which the magnetic field is zero) relative to the ideal machine axis, and 2) coupling between the horizontal and vertical planes proportional to the roll of the magnetic field relative to the machine plane. Realignments (the HL-LHC has full remote alignment capabilities) can correct both transverse and roll offsets, but the available motion is limited by acceptable bellows deformation. Bellows also need to accommodate manufacturing imperfections, and production is not yet complete [7]. Here, we assume that transverse offsets can be up to 0.5 mm and roll offsets below 1 mrad. Orbit correctors can compensate for offset deviations to the extent that the errors are below 0.5 mm [8].

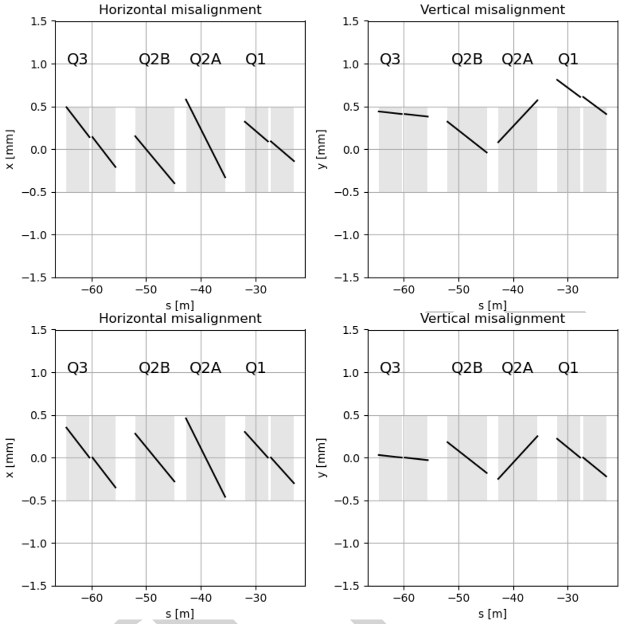

Figure 1: Expected magnetic-axis misalignment in the IT string before (top) and after correction (bottom). Grey boxes show the triplet-gradient locations used to identify the error sources.

Driving orbit correctors to their maximum strengths, however, is not desirable since their field quality deteriorates at large currents in both planes (orbit correctors are dual-plane nested correctors in the common-pipe region [9] and dual-plane 2-in-1 correctors in the two-pipe regions [10]). Roll deviations in the triplet can also be corrected with local and global coupling correctors; however, relying on global correctors implies either having coupling at the IP, which reduces luminosity, or coupling in the triplets, which enhances nonlinear coupling effects. In addition, starting commissioning with strong coupling inevitably increases commissioning time. Given these premises, the best strategy is to use the magnetic measurements to install the magnets with the best-aligned magnetic axes and to preset the orbit and coupling corrections during the first commissioning using the model.

As proof of principle, Figures 1 and 2 illustrate the strategy adopted to correct imperfections for the IT string installation [11]. The measured magnetic axis, transferred to the machine plane, results in a large orbit error and orbit-corrector usage. A complete correction of the axis, including the slopes, would result in excessive offsets in the bellows. A compromise solution [12], compensating only for the average axis correction, shows almost negligible orbit error and orbit-corrector usage while preserving the bellows range.

Measured roll deviations reached 2.5 mrad [7]. Uncompensated, they would require about half the available skew-

---

* riccardo.de.maria@cern.ch

[1] In the past, magnetic measurements could not be reconciled with optics measurements [6]

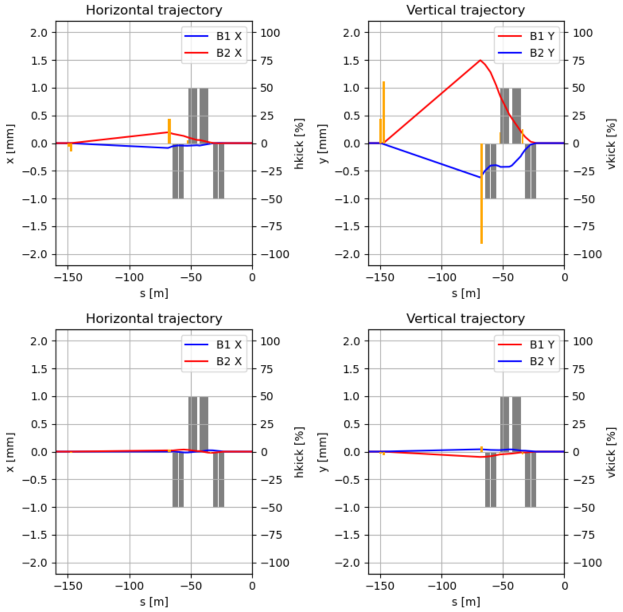

Figure 2: Expected trajectory and orbit-corrector powering in the IT string before (top) and after correction (bottom). Orange bars show corrector kicks in percent of available strength, using the right axis; grey boxes show the triplet-gradient locations.

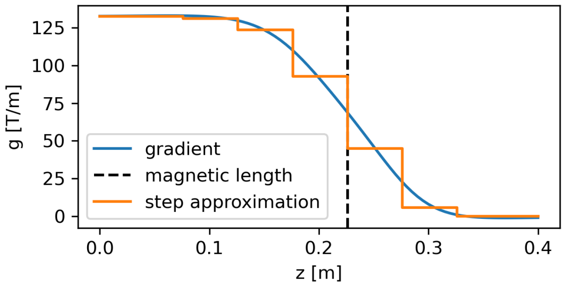

Figure 3: Fringe-field approximation used for optics calculation. The roll-off is obtained from a Roxie model [13].

quadrupole strength; the IT string construction, however, allowed installation with the magnetic axis corrected [7].

Table 1: Extracted parameters from magnetic-length and transfer-function measurements. The quoted value is the measurement average; uncertainties are upper and lower bounds due to the small sample size.

MQXA	**Nominal**	**Measurement**
Magnetic length [m]	4.213	$4.212^{+0.001}_{-0.002}$
Gradient [T/m]	132.6	$133.1^{+0.2}_{-0.3}$
Gradient slope [mT/(A m)]	8.17	$7.59^{+0.01}_{-0.02}$
Int. gradient [T]	558.6	$560.9^{+0.8}_{-1.3}$
Int. gradient slope [mT/A]	34.4	$32.98^{+0.06}_{-0.08}$
MQXB	**Nominal**	**Measurement**
Magnetic length [m]	7.172	$7.179^{+0.005}_{-0.003}$
Gradient [T/m]	132.6	$132.5^{+0.2}_{-0.2}$
Gradient slope [mT/(A m)]	8.17	$7.55^{+0.03}_{-0.02}$
Int. gradient [T]	951	$951.1^{+1.7}_{-1.3}$
Int. gradient slope [mT/A]	58.6	$54.2^{+0.2}_{-0.1}$

Table 2: Impact of imperfections on beta-beating: a) maximum beta-beating for uncorrected optics; b) maximum beta-beating in the interaction region for a measured model matched at the IP; c) beta-beating at the IP for a measured model matched at the BPMs with nominal optics as reference. Values are for Beam 1, end-of-leveling optics with $\beta^* = 15$ cm. The last three cases use the maximum beta-beating from a small Monte Carlo sample; "unst." denotes unstable optics.

Imperfection	**a [%]**	**b [%]**	**c [%]**
Fringe fields	17	0.01	0.005
Magnetic length systematic	28	0.04	0.017
Magnetic length spread	2	0.01	0.007
Transfer-function spread	unst.	0.12	0.12
Longitudinal misalignment	8	0.004	0.005

OPTICS DEVIATIONS

The following MQXFA and MQXFB imperfections are expected to measurably affect the optics and should therefore be considered to facilitate commissioning: a) Fringe fields [14] have a measurable impact on the optics. Figure 3 shows the fringe model, based on magnet simulation, which is used in the following estimates; b) Magnetic-length deviations can be estimated from the measurements of the first quadrupoles; see Fig. 4 and Table 1. The values show a relative spread of about $6 \cdot 10^{-4}$ for both magnet types and a systematically longer length for the MQXFB. c) Transfer-function deviations can be estimated from the measurements of the first quadrupoles; see Fig. 5 and Table 1. The results show a systematically larger field for the MQXFA, a relative spread of about $22 \cdot 10^{-4}$ for the gradient, and a slightly smaller relative deviation of $17 \cdot 10^{-4}$ when considering the integrated field. d) Longitudinal misalignments of the quadrupoles have been estimated to be up to 5 mm [15], of the same order of magnitude as the magnetic-length uncertainty. Note that some error sources are neglected here as e.g. magnetic uncertainties, errors in the IR dipoles and orbit correctors, non-linear fields, orbit offsets, and energy errors.

The end-of-leveling optics is so sensitive to optics imperfections, due to the large β-functions, that any minimal uncorrected imperfection translates into large beta-beating. At the same time, the triplet magnets and Q4 have enough degrees of freedom to restore the nominal optics transport between the IP and Q4. If we include the Q1A trim, which today is limited to performing k-modulation measurements [16], the triplet system has enough degrees of freedom to restore the optics transport within the triplet region. Clearly, having the possibility to fully correct the

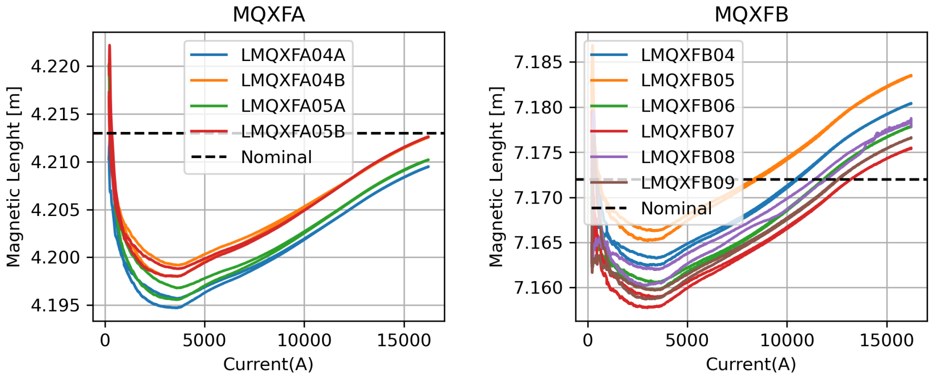

Figure 4: Magnetic-length measurements for the MQXFA and MQXFB magnets as a function of current. Nominal values are used in nominal optics models.

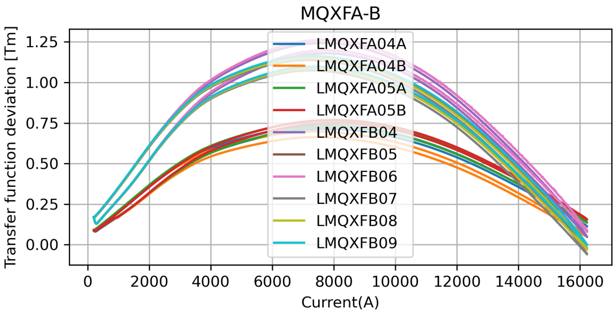

Figure 5: Transfer-function measurements of the MQXFA and MQXFB magnets: deviation between the integrated B_2 component measured at the reference radius of 50 mm and the nominal linear function $B_{2,\mathrm{nom}} L_{\mathrm{nom}} \frac{I}{I_{\mathrm{nom}}}$.

optics does not mean that the correction is feasible, given the accuracy of the BPMs, their positions, and the accuracy of the k-modulation measurements. In particular, β^* is not an easily measurable quantity, and the accuracy of its determination depends on the uncertainty of the machine model [17], which is not addressed here. Finally, the correction process takes time, on the order of days, and is therefore very expensive. The closer the model is to the real machine, the shorter the time it will take to converge to the nominal optics [18].

It is interesting to compare the uncorrected and fully corrected optics errors for the different imperfections mentioned above to understand their relative importance, as summarised in Table 2. The transfer-function spread is the dominant imperfection, followed by the systematic magnetic-length deviation and fringe fields. The other imperfections have a smaller impact on the optics. The transfer-function spread is large enough to require correction before reaching the low-β^* optics (10^{-4} deviations already give 20 % beta-beating), and including it from the beginning should, therefore, reduce the commissioning time. The beta-beating for optics matched at the IP (second column) shows how close the nominal model is to a realistic model after an ideal correction. The values are very small and well within the expected measurement errors. The third column shows the error at the IP if the nominal model is taken as a reference for correction. These errors are also very small and acceptable for any correction strategy. The implication is that a well-corrected machine will have no significant beta-beating residuals either at the IP or in the triplet region, even if the nominal model is used as a reference for the correction. The advantage of using a realistic model is, therefore, to reduce the initial optics errors and the number of iterations needed during commissioning.

CONCLUSION

We collected the available measurements of the magnetic axis deviations, magnetic lengths, and transfer functions of the first quadrupoles produced for the inner triplets and used them to build a more accurate commissioning model of the machine. The knowledge of magnetic axis deviations is essential to pre-align the magnetic axis and enable commissioning with a well-corrected orbit and coupling. The uncertainty on the magnetic-axis deviations should be well below the deviations observed in the initial production. An uncompensated installation would likely require corrector strengths beyond the acceptable limits. Knowledge of the magnetic lengths, transfer functions, and longitudinal positions also helps build models that more closely reflect reality. We show that the optics errors are dominated, in order, by transfer-function spread, systematic magnetic-length deviation, fringe fields, magnetic-length spread, and finally longitudinal misalignment. A model including alignment and magnetic measurements allows starting the beam commissioning with optics in the triplet region that already includes the imperfections that would otherwise need to be corrected; however, this is not sufficient to eliminate the need for corrections given the observed sensitivity to deviations and the uncertainties in the magnetic measurements (in particular, on the transfer function). Once the ideal correction is performed, the realistic models studied here remain within 1 % beta-beating relative to the nominal model (note that magnetic uncertainties and several error sources are neglected). We therefore plan to provide optics models that incorporate the measured imperfections to reduce the beam commissioning time.

REFERENCES

[1] S. Fartoukh, F. Cerutti, M. Hostettler, and S. Kostoglou, “LHC machine configuration evolution over Run 3 for maximised performance and inner triplet lifetime”, presented at IPAC’26, Deauville, France, May 2026, paper MOP1057, this conference,

[2] J. Gray, K. Skoufaris, R. D. Maria, R. Tomas, and Y. Angelis, “Design challenges and solutions for flat optics in HL-LHC”, presented at IPAC’26, Deauville, France, May 2026, paper MOP1067, this conference,

[3] E. Maclean *et al.*, “Probing the ultimate beta* reach of the LHC”, presented at IPAC’26, Deauville, France, May 2026, paper MOP1066, this conference,

[4] M. Stefanelli, Y. Angelis, J. Dilly, J. Gray, E. Maclean, and F. Soubelet, “Extrapolated optics measurement from BPM to instrumentation in LHC commissioning”, presented at IPAC’26, Deauville, France, May 2026, paper WEP5072, this conference,

[5] “High-Luminosity Large Hadron Collider (HL-LHC): Technical Design Report V. 0.1”, CERN, CERN-2017-007-M, 2017. doi:10.23731/CYRM-2017-004

[6] T. Persson *et al.*, “LHC optics commissioning: a journey towards 1% optics control”, *Phys. Rev. Accel. Beams*, vol. 20, no. 6, p. 061002, Jun. 2017. doi:10.1103/PhysRevAccelBeams.20.061002

[7] R. De Maria *et al.*, “Impact of magnetic-mechanical deviations and their measurements”, 15th HL-LHC Collaboration Meeting, `https://indico.cern.ch/event/1559978/contributions/6664973/`, 2025,

[8] D. Gamba and R. D. Maria, “IP Orbit Correction Update for HL-LHC”, in *Proc. IPAC’18*, Vancouver, Canada, Apr.-May 2018, pp. 3048–3051. doi:10.18429/JACoW-IPAC2018-THPAF039

[9] M. Domínguez *et al.*, “Field quality of the series of short orbit nested corrector magnets for hl-lhc”, *IEEE Trans. Appl. Supercond.*, vol. 36, no. 3, pp. 1–5, 2026. doi:10.1109/TASC.2025.3624733

[10] V. Ilardi *et al.*, “Fabrication and test of the fourth prototype of the d2 orbit corrector dipole for hl-lhc”, *IEEE Trans. Appl. Supercond.*, vol. 34, no. 5, pp. 1–6, 2024. doi:10.1109/TASC.2023.3343674

[11] M. B. Bajko *et al.*, “The Inner Triplet String Facility for HL-LHC: Design and Planning”, in *Proc. IPAC’21*, Campinas, Brazil, May 2021, pp. 3592–3595. doi:10.18429/JACoW-IPAC2021-WEPAB376

[12] R. De Maria, “Misalignments shifts for IT String: Process, results and follow-ups”, Alignment WG meeting #82, `https://indico.cern.ch/event/1525688/contributions/6418074/`,

[13] S. I. Bermudez, “Roxie 3D field map”, Private communication, 2012,

[14] B. J. Holzer *et al.*, “Study of the Impact of Fringe Fields of the Large Aperture Triplets on the Linear Optics of the HL-LHC”, in *Proc. IPAC’13*, Shanghai, China, May 2013, paper WEPEA059, pp. 2642–2644. `https://jacow.org/IPAC2013/papers/WEPEA059.pdf`

[15] R. De Maria, “Alignment and Mechanical Tolerances for HL-LHC in Point 1 and 5”, EDMS 2458050/1.0, `https://edms.cern.ch/document/2458050/1.0`,

[16] R. Tomás, M. Aiba, A. Franchi, and U. Iriso, “Review of linear optics measurement and correction for charged particle accelerators”, *Phys. Rev. Accel. Beams*, vol. 20, no. 5, p. 054801, May 2017. doi:10.1103/PhysRevAccelBeams.20.054801

[17] J. Coello de Portugal, R. Tomás, and M. Hofer, “New local optics measurements and correction techniques for the lhc and its luminosity upgrade”, *Phys. Rev. Accel. Beams*, vol. 23, no. 4, p. 041001, Apr. 2020. doi:10.1103/PhysRevAccelBeams.23.041001

[18] X. Buffat *et al.*, “Optics Measurement and Correction Strategies for HL-LHC”, CERN, Geneva, Rep., 2022. `https://cds.cern.ch/record/2808650`